

Band gap effects of hexagonal boron nitride using oxygen plasma

Singh, Ram Sevak; Tay, Roland Yingjie; Chow, Wai Leong; Tsang, Siu Hon; Mallick, Govind; Teo, Edwin Hang Tong

2014

Singh, R. S., Tay, R. Y., Chow, W. L., Tsang, S. H., Mallick, G., & Teo, E. H. T. (2014). Band gap effects of hexagonal boron nitride using oxygen plasma. *Applied Physics Letters*, 104(16), 163101-.

<https://hdl.handle.net/10356/97555>

<https://doi.org/10.1063/1.4872318>

© 2014 AIP Publishing LLC. This paper was published in *Applied Physics Letters* and is made available as an electronic reprint (preprint) with permission of AIP Publishing LLC. The paper can be found at the following official DOI: [<http://dx.doi.org/10.1063/1.4872318>]. One print or electronic copy may be made for personal use only. Systematic or multiple reproduction, distribution to multiple locations via electronic or other means, duplication of any material in this paper for a fee or for commercial purposes, or modification of the content of the paper is prohibited and is subject to penalties under law.

Downloaded on 20 Mar 2024 20:14:43 SGT

Band gap effects of hexagonal boron nitride using oxygen plasma

Ram Sevak Singh, Roland Yingjie Tay, Wai Leong Chow, Siu Hon Tsang, Govind Mallick, and Edwin Hang Tong Teo

Citation: [Applied Physics Letters](#) **104**, 163101 (2014); doi: 10.1063/1.4872318

View online: <http://dx.doi.org/10.1063/1.4872318>

View Table of Contents: <http://scitation.aip.org/content/aip/journal/apl/104/16?ver=pdfcov>

Published by the [AIP Publishing](#)

Articles you may be interested in

[High quality single atomic layer deposition of hexagonal boron nitride on single crystalline Rh\(111\) four-inch wafers](#)

Rev. Sci. Instrum. **85**, 035101 (2014); 10.1063/1.4866648

[Effects of Ag-induced acceptor defects on the band gap tuning and conductivity of Li:ZnO films](#)

J. Appl. Phys. **113**, 203518 (2013); 10.1063/1.4807932

[Valence band offset at the amorphous hydrogenated boron nitride-silicon \(100\) interface](#)

Appl. Phys. Lett. **101**, 042903 (2012); 10.1063/1.4739474

[Low threshold field emission from high-quality cubic boron nitride films](#)

J. Appl. Phys. **111**, 093728 (2012); 10.1063/1.4711093

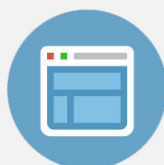
[A comparison of plasma-activated N₂/O₂ and N₂O₂ mixtures for use in ZnO:N synthesis by chemical vapor deposition](#)

J. Appl. Phys. **96**, 7036 (2004); 10.1063/1.1804614



Re-register for Table of Content Alerts

Create a profile.



Sign up today!



Band gap effects of hexagonal boron nitride using oxygen plasma

Ram Sevak Singh,^{1,a)} Roland Yingjie Tay,^{1,2} Wai Leong Chow,¹ Siu Hon Tsang,² Govind Mallick,^{2,3} and Edwin Hang Tong Teo^{1,4,b)}

¹*School of Electrical and Electronic Engineering, Nanyang Technological University, 50 Nanyang Avenue, Singapore 639798, Singapore*

²*Temasek Laboratories@NTU, 50 Nanyang Avenue, Singapore 639798, Singapore*

³*Weapons and Materials Research Directorate, U.S. Army Research Laboratory, Aberdeen Proving Ground, Maryland 21005, USA*

⁴*School of Materials Science and Engineering, Nanyang Technological University, 50 Nanyang Avenue, Singapore 639798, Singapore*

(Received 25 January 2014; accepted 9 April 2014; published online 21 April 2014)

Tuning of band gap of hexagonal boron nitride (h-BN) has been a challenging problem due to its inherent chemical stability and inertness. In this work, we report the changes in band gaps in a few layers of chemical vapor deposition processed as-grown h-BN using a simple oxygen plasma treatment. Optical absorption spectra show a trend of band gap narrowing monotonically from 6 eV of pristine h-BN to 4.31 eV when exposed to oxygen plasma for 12 s. The narrowing of band gap causes the reduction in electrical resistance by ~ 100 fold. The x-ray photoelectron spectroscopy results of plasma treated hexagonal boron nitride surface show the predominant doping of oxygen for the nitrogen vacancy. Energy sub-band formations inside the band gap of h-BN, due to the incorporation of oxygen dopants, cause a red shift in absorption edge corresponding to the band gap narrowing. © 2014 AIP Publishing LLC. [<http://dx.doi.org/10.1063/1.4872318>]

Two-dimensional (2D) hexagonal boron nitride (h-BN) materials have received enormous interests due to its intriguing electronic, thermal, and mechanical properties.¹ Due to the similarity in lattice constants, the hybridized structures of h-BN and graphene can be used as composite electronic devices.^{2,3} Since, h-BN is an insulator with a large direct band gap of almost 6 eV,⁴ there has been a great deal of interest from physicists, chemists, material scientists, and engineers to reduce and/or to manipulate the energy to achieve desired future electronic applications. Energy gap of h-BN can be tuned using various strategies, including atomic doping, composites, and surface functionalization.^{2,5,6} Recently, it was predicted that optical, electrical, and magnetic properties of boron nitride can be tuned by oxygen substitution using theoretical calculations.⁷⁻⁹ In this Letter, we present our observations of band gap narrowing in a few layers of h-BN with respect to doping of oxygen atoms into the lattice of h-BN via a simple, economical, and environmentally safe method of oxygen plasma treatment. Though, there have been a few attempts to alternate the h-BN band gap using carbon doping² and through hydrogenation,¹⁰ experimental observation of oxygen induced reduction of the gap is not reported. Optical absorption measurements exhibit a monotonically narrowing of band gap in oxygen plasma treated h-BN samples, indicating the decrease in magnitude with increase of oxygen concentration. Furthermore, the decrease of band gap results in a reduction (~ 100 fold) of electrical resistance of oxygen doped h-BN films as substantiated by electrical measurements. X-ray photoelectron spectroscopy (XPS) suggests that h-BN under O₂-plasma undergoes the changes in surface

structure by creation of nitrogen (N) vacancies enabling the substitution of N-sites by oxygen atoms. This is generally symbolized as O_N-substitution doping. Tunable band gap of h-BN, realized in this study, could be a platform towards applications in nano- or opto-electronic devices.

h-BN used in this study was prepared by chemical vapor deposition (CVD) on copper substrate (25 μm thick, purchased from Alfa Aesar) using ammonia borane (Sigma Aldrich) as precursor.^{11,12} Prior to the deposition, copper substrate was submerged into dilute nitric acid followed by rinsing it using deionized (DI) water. Synthesis of h-BN involved annealing of copper substrate with two major steps: (1) Cu substrate was heated to 800 °C for 20 min in Ar/H₂ (425:75 sccm), and (2) it was gradually heated up to 1050 °C for 40 min under the vapor of ammonia borane. 5 mg of the precursor, ammonia borane, was placed in a ceramic holder within the quartz tube and was heated at 60 °C with a flexible heating belt to vaporize it. As-grown h-BN on copper substrate was investigated using scanning electron microscopy (SEM; LEO 1550 Gemini) as shown in Fig. 1(a). In order to determine the thickness, the synthesized h-BN was transferred onto SiO₂ (285 nm)/Si substrate.¹³ A thin layer of poly(methyl methacrylate) (PMMA) was spin-coated on top of the h-BN/Cu substrate, baked at 105 °C for 2 min, and subsequently put on Fe(NO₃)₃ solution for few hours to etch away the Cu. The free standing PMMA coated h-BN was then rinsed in DI water for several times and extracted onto SiO₂/Si or quartz substrate. Finally, the sample was submerged in acetone to remove the PMMA. Atomic force microscopy (AFM) was used to determine the thickness of as-grown h-BN films. Fig. 1(b) shows an AFM image of a continuous h-BN film on SiO₂/Si substrate with measured thickness of 1.89 nm.

Ultraviolet-visible (UV-Vis) spectroscopy is a powerful tool to investigate the optical properties such as absorption, transmittance, and optical band gap of materials. In order to

^{a)}Current address: Department of Physics, National Institute of Technology, Kurukshetra 136119 (Haryana), India.

^{b)}Author to whom correspondence should be addressed. Electronic mail: hteoo@ntu.edu.sg

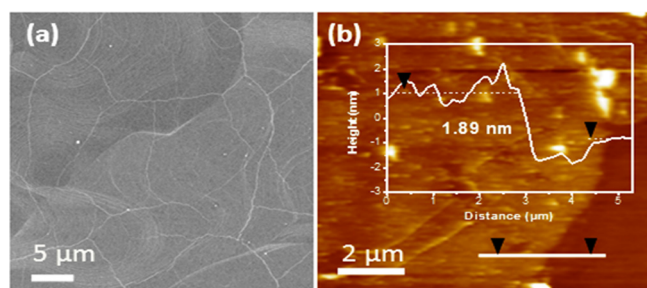


FIG. 1. Characterizations of as-synthesized h-BN. (a) SEM image showing a continuous film of h-BN. (b) AFM image of h-BN film. The inset shows a height profile, indicating the thickness of the h-BN film.

conduct UV-vis absorption measurements, the h-BN film was transferred on optical quartz substrate from copper substrate using the methods described above. Two identical quartz substrates were used for base line corrections. The measurements were conducted by a UV-Vis (Shimadzu UV-2450) system at room temperature and in ambient conditions.

The h-BN sample was exposed to oxygen plasma cumulatively for 3 s, 6 s, and 12 s. The experiments were carried out using a commercial plasma system (AST Clen100 Descum) with RF power of 25 W. O₂-plasma was chosen for oxygen substitution because atomic oxygen can generate and directly substitute nitrogen atom at a site where a B–N bond is broken. Since, the binding energy of a hexagonal B–N bond is 7–8 eV,¹⁴ sufficient number of electrons or ions of at least this amount of energy is needed to break these bonds while adjusting the total energy so as to minimize the damage to the surface of h-BN. O₂-plasma treatment over ultrathin few layers of h-BN is a crucial process. We managed to implement this by using low power (25 W) and varying the exposure time of the plasma. The power used in our study can be considered “mild” as compared to the power (100 W) used previously for BN nanotubes.⁸ Furthermore, this power (25 W) is sufficient to generate ions with its bombardment energy >10 eV, which is strong enough to break a B–N bond in a h-BN system. The effect of O₂-plasma modification over h-BN films was investigated using UV-Vis spectroscopy, electrical resistance measurements, and XPS.

Fig. 2 shows the UV-Vis absorption spectra acquired from O₂-plasma treated h-BN films corresponding to exposure times of 3 s, 6 s, and 12 s, respectively. The inset shows the spectrum obtained from a pristine (before exposure) h-BN sample. The spectrum of the pristine h-BN shows a

prominent absorption at round 202 nm which is the result of inter-band transition from valence to conduction band of the h-BN. This absorption band relates to the optical band gap in h-BN. Under O₂-plasma, it is evident that the spectrum undergoes significant changes in absorption edges, indicating a band gap narrowing in h-BN. h-BN is a direct band gap semiconductor and the derived formula to estimate its band gap is given by its absorption coefficient¹⁵

$$\alpha = C(E - E_g)^{1/2}/E, \quad (1)$$

where $\alpha = A/d$ (A is the optical absorption measured by the UV-visible spectroscopy and d is the thickness of the film), C is a constant, and E , the photo energy, is calculated by $E = hc/\lambda$, where h is the plank's constant and λ is the wavelength. Based on the above Eq. (1), a plot of $(\alpha E)^2$ vs. E (Tauc's plot) can be generated. The extrapolations of the curves intersecting the x-axis, when $(\alpha E)^2 = 0$, corresponds to the estimated value of the band gap, E_g . Tauc plots, corresponding to Fig. 2(a), are presented in Fig. 2(b). It is clear that, compared to the pristine h-BN (band gap = 6 eV), O₂-plasma treated samples show a reduction of band gap from 6 to 4.31 eV at 12 s which increase as the exposure is decreased. The estimated band gaps vs. plasma exposure times are presented in Fig. 3. The narrowing effects of the optical band gap in the absorption spectrum can be understood based on the chemical doping of h-BN lattice. The chemical doping of h-BN can result in the formation of doping energy level inside the energy gap of h-BN, which dramatically causes a red shift in absorption spectrum corresponding to band gap narrowing. It is also observed that band gap narrowing phenomenon saturates at exposure time of 12 s (Fig. 3) at 4.31 eV when 25 W RF power is used, as oxygen substitution predominantly occurs in the early stages during O₂-plasma treatment. Although increasing RF power is able to break more B–N bonds, too much power will cause severe etching of the film.

To obtain more insight into the chemical structure and mechanism of oxygen doping into h-BN, XPS measurements on h-BN samples before (pristine or untreated h-BN) and after O₂-plasma exposure were conducted. The measurements were carried out using a VG ESCA 220i-XL Imaging XPS. Monochromatic Al K α X-ray ($h\nu = 1486.6$ eV) was employed for analysis with photoelectron take-off angle of 90° with respect to surface plane. The analysis area was approximately

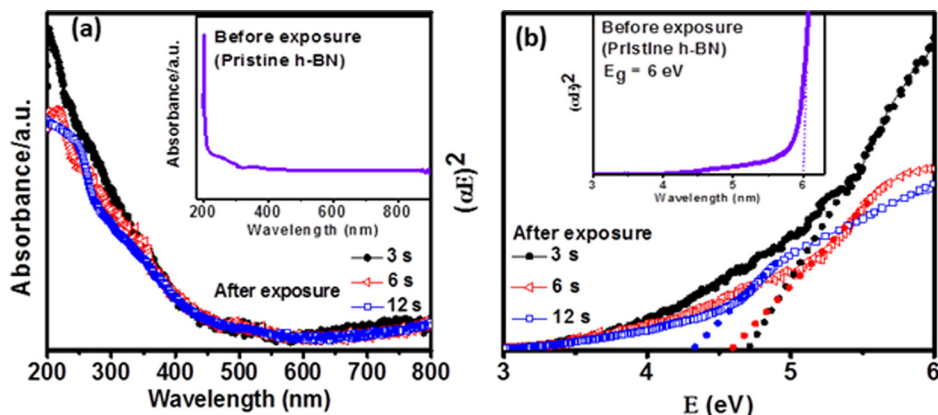


FIG. 2. (a) UV-Vis absorption spectra acquired from h-BN samples exposed to O₂-plasma for 3 s, 6 s, and 12 s, respectively. The inset shows the spectrum of pristine (before exposure) h-BN sample. (b) Tauc's plots obtained from (a) for the determination of band gaps.

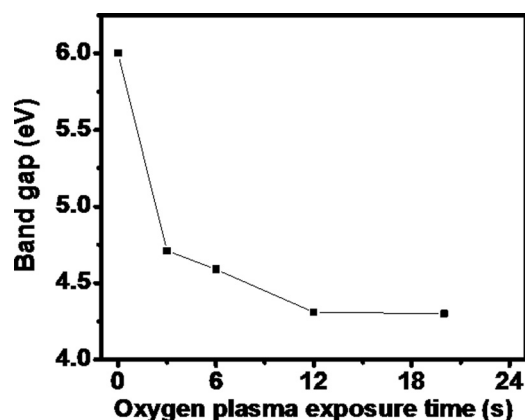


FIG. 3. A plot showing the change in band gap of h-BN with respect to oxygen plasma exposure time.

700 μm in diameter while the maximum analysis depth lay in the range of 4–8 nm. Charge correction was made based on adventitious C1s (C-C/C-H) at 285.0 eV using standard software. For chemical state analysis, a spectral deconvolution was performed by a curve-fitting procedure based on Lorentzian broadened by a Gaussian. The XPS N1s and B1s spectra of the h-BN before and after exposure to O_2 -plasma are shown in Fig. 4. Before exposure, B1s spectrum (Fig. 4(e)) shows a peak at 190.7 eV (Ref. 8) with a very weak additional peak, labelled “ BO_xN_y ” at higher energy

(191.8 eV). After exposure, a pronounced peak of BO_xN_y at 191.8 eV was observed (Fig. 4(f)). This BO_xN_y peak corresponds to boron atoms bound to oxygen atoms (replacement of nitrogen) as labeled in the schematic diagram in Fig. 4(b). Substitution doping mechanism was confirmed in our analysis by analysing the N1s (398.3 eV) and B1s (190.7 eV) spectra before (Figs. 4(c) and 4(e)) and after exposure (Figs. 4(d) and 4(f)). After O_2 -plasma exposure, it was observed that total number of B changed a little, while content of N was reduced indicating the creation of nitrogen vacancy (V_N) accompanied by an increase in oxygen content. The relative compositional change (substrate related elements or chemical states are excluded) in h-BN before and after exposure is presented in Table I. As such, the observations suggest that the oxygen plasma breaks the B–N bond to create the V_N where an oxygen atom is replaced. This phenomenon is supported by the theoretical works^{9,16,17} where O substitution for N is more favorable due to the lower formation energy.

For electrical measurements, h-BN devices were fabricated using photolithography process, metal deposition, and oxygen plasma etching. Two Cr (10 nm)/Au (50 nm) metal electrodes were deposited using electron beam evaporator. To define the channel, h-BN film was etched under oxygen plasma. The fabricated h-BN device, in this study, is shown in the inset of Fig. 5. We performed the electrical resistance measurements of pristine h-BN device before and after exposing to oxygen plasma for the duration of 3 s, 6 s, and

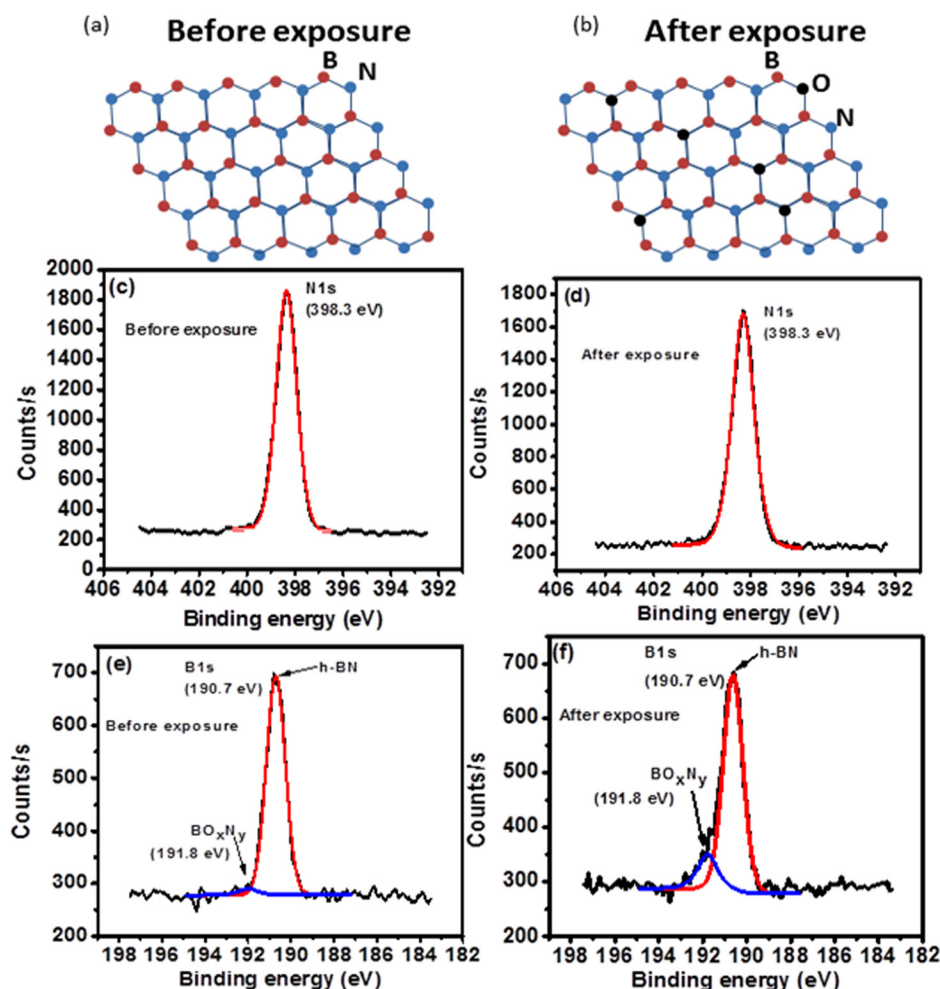


FIG. 4. Chemical structure of untreated (before exposure to O_2 -plasma) and treated (after exposure) h-BN samples. A schematic showing the structure of h-BN (a) before exposure, and (b) with oxygen doping after exposure. (c) XPS N1s spectrum before exposure. (d) XPS N1s spectrum after exposure. (e) XPS B1s before exposure. (f) XPS B1s spectrum after exposure.

TABLE I. Chemical states and composition of B and N elements.

| Elements | Before exposure | | After exposure | |
|-----------------------------|-------------------------|------------------------|-------------------------|------------------------|
| | E_b (eV \pm 0.2) | Composition (at. %) | E_b (eV \pm 0.2) | Composition (at. %) |
| B1s h-BN | 190.7 | 26.2 | 190.7 | 22.5 |
| B1s BO_xN_y | 191.8 | 0.8 | 191.8 | 3.8 |
| N1s h-BN | 398.3 | 25.8 | 398.3 | 23.7 |

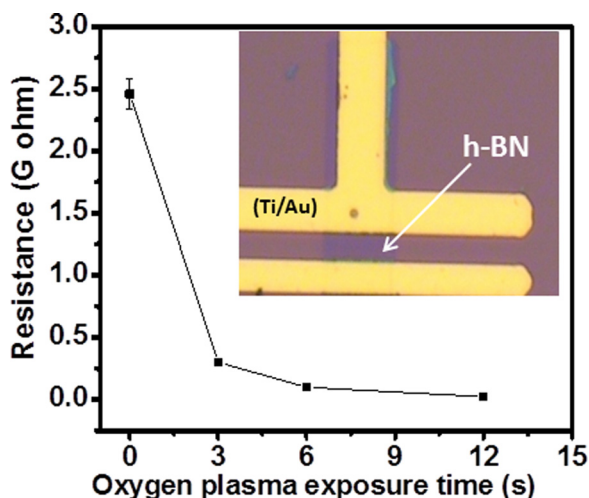


FIG. 5. Electrical resistance of h-BN film measured at different O_2 -plasma exposure times. The inset shows an h-BN device with two metal (Ti/Au) electrodes for electrical resistance measurements.

12 s, respectively. All the measurements were conducted at room temperature and at ambient conditions using Keithley 4200 semiconductor characterization system. Fig. 5 shows the measured resistances of h-BN with respect to oxygen plasma exposure times. It is evident that h-BN under O_2 -plasma undergoes a change in resistance from 2.4 GΩ (0 s or pristine h-BN) to 0.02 GΩ (sample exposed for 12 s) which is ~ 100 fold reduction in resistance compared to unexposed h-BN sample. The reduction in resistance due to oxygen doping is the indication of a band gap narrowing phenomenon in h-BN. The resistance of 0.02 GΩ observed is due to the saturated 4.31 eV energy gap at 12 s. Nonetheless, the trend of cumulative reduction in resistance supports our observations of optical band gap narrowing effects in UV-Vis spectra (Fig. 2).

In summary, the narrowing of band gap in a CVD grown h-BN using oxygen plasma treatment is realized. Optical absorption spectra show a reducing band gap trend from 6 eV of pristine h-BN to 4.31 eV of h-BN exposed for the duration of 12 s. The narrowing of band gap is also responsible for the reduction in electrical resistance (~ 100 fold) of exposed h-BN film. XPS measurements reveal that h-BN under O_2 -plasma undergoes the breaking of B-N bond, creating nitrogen vacancy followed by oxygen doping. This chemical doping of h-BN results in the formation of a sub-band inside the band gap and causes a red shift in absorption edge corresponding to the band gap narrowing. The study could be promising to modulate the electronic, magnetic, and optical property of h-BN material towards future nano-electronic device applications.

The authors acknowledge the support from NOVITAS, Nanoelectronics Center of Excellence, Nanyang Technological University.

- ¹Y. Kubota, K. Watanabe, O. Tsuda, and T. Taniguchi, *Science* **317**(5840), 932 (2007).
- ²L. Ci, L. Song, C. Jin, D. Jariwala, D. Wu, Y. Li, A. Srivastava, Z. F. Wang, K. Storr, L. Balicas, F. Liu, and P. M. Ajayan, *Nature Mater.* **9**(5), 430 (2010).
- ³K. Suenaga, C. Colliex, N. Demoncy, A. Loiseau, H. Pascard, and F. Willaime, *Science* **278**(5338), 653 (1997).
- ⁴K. Watanabe, T. Taniguchi, and H. Kanda, *Nature Mater.* **3**(6), 404 (2004).
- ⁵W. Q. Han, L. Wu, Y. Zhu, K. Watanabe, and T. Taniguchi, *Appl. Phys. Lett.* **93**(22), 223103 (2008).
- ⁶Y. J. Cho, C. H. Kim, H. S. Kim, J. Park, H. C. Choi, H. J. Shin, G. Gao, and H. S. Kang, *Chem. Mater.* **21**(1), 136 (2009).
- ⁷G. Gou, B. Pan, and L. Shi, *J. Am. Chem. Soc.* **131**(13), 4839 (2009); L. Liu, T. K. Sham, and W. Han, *Phys. Chem. Chem. Phys.* **15**(18), 6929 (2013).
- ⁸X. J. Dai, Y. Chen, Z. Chen, P. R. Lamb, L. H. Li, J. Plessis, D. G. McCulloch, and X. Wang, *Nanotechnology* **22**(24), 245301 (2011).
- ⁹J. Wu and W. Zhang, *Solid State Commun.* **149**(11), 486 (2009).
- ¹⁰H. X. Zhang and P. X. Feng, *ACS Appl. Mater. Interfaces* **4**(1), 30 (2012).
- ¹¹R. Y. Tay, X. Wang, S. H. Tsang, G. C. Loh, R. S. Singh, H. Li, G. Mallick, and E. H. T. Teo, *J. Mater. Chem. C* **2**(9), 1650 (2014).
- ¹²R. Y. Tay, M. H. Griep, G. Mallick, S. H. Tsang, R. S. Singh, T. Tumlin, E. H. T. Teo, and S. P. Karna, *Nano Lett.* **14**(2), 839 (2014).
- ¹³X. Li, Y. Zhu, W. Cai, M. Borysiak, B. Han, D. Chen, R. D. Piner, L. Colombari, and R. S. Ruoff, *Nano Lett.* **9**(12), 4359 (2009).
- ¹⁴N. Ooi, A. Rairkar, L. Lindsley, and J. B. Adams, *J. Phys.: Condens. Matter* **18**(1), 97 (2006).
- ¹⁵T. H. Yuzuriha and D. W. Hess, *Thin Solid Films* **140**(2), 199 (1986).
- ¹⁶L. A. Silva, S. C. Guerini, and V. Lemos, *IEEE Trans. Nanotechnol.* **5**(5), 517 (2006).
- ¹⁷Z. F. Zhang, T. G. Zhou, and X. Zuo, *Acta Phys. Sin.* **62**(8), 83102 (2013).